Robust Registration Method for Interventional MRI-Guided Thermal Ablation of Prostate Cancer

Baowei Fei [a*], Andrew Wheaton [a], Zhenghong Lee [b], Kenichi Nagano [a]
Jeffrey L Duerk [b a], David L Wilson [a b**]
[a] Department of Biomedical Engineering, Case Western Reserve University, OH 44106
[b] Department of Radiology, University Hospitals of Cleveland, OH 44106

ABSTRACT

We are investigating methods to register live-time interventional magnetic resonance imaging (iMRI) slice images with a previously obtained, high resolution MRI image volume. The immediate application is for iMRI-guided treatments of prostate cancer. We created and evaluated a slice-to-volume mutual information registration algorithm for MR images with special features to improve robustness. Features included a multi-resolution approach and automatic restarting to avoid local minima. We acquired 3D volume images from a 1.5 T MRI system and simulated iMRI images. To assess the quality of registration, we calculated 3D displacement on a voxel-by-voxel basis over a volume of interest between slice-to-volume registration and volume-to-volume registrations that were previously shown to be quite accurate. More than 500 registration experiments were performed on MR images of volunteers. The slice-to-volume registration algorithm was very robust for transverse slice images covering the prostate. A 100% success rate was achieved with an acceptance criterion of < 1.0 mm displacement error over the prostate. Our automatic slice-to-volume mutual information registration algorithm is robust and probably sufficiently accurate to aid in the application of iMRI-guided thermal ablation of prostate cancer.

Keywords: Image registration, mutual information, magnetic resonance imaging (MRI), interventional MRI, prostate cancer, minimally invasive treatment, thermal ablation.

1. INTRODUCTION

We are investigating methods for registering slice images obtained on a low field iMRI system to high-resolution MR volumes obtained on a traditional 1.5 T scanner. Immediate applications involve the treatment of prostate cancer as described below. To be useful for an interventional procedure, a registration method must be automatic, accurate, robust, and fast. Currently, we are investigating voxel-based methods because of their ease of use and reported accuracy for other applications.

There are important reasons for this investigation. At our institution, we have extensive experience with minimally invasive treatment of abdominal cancer using iMRI-guided radiofrequency thermal abaltion.[1,2,3] In the case of the prostate, the tumor is not reliably identified with MR. Hence, other functional imaging techniques are required, and potential methods include SPECT antibody imaging and MR spectroscopy. To incorporate the functional images with iMRI tumor targeting, one can first register the low-resolution functional images with a high-resolution MRI. Then by registering the high-resolution MR volume with live-time iMRI acquisitions, we can map both the functional data and high-resolution anatomic information to live-time iMRI images for improved tumor targeting. Image guided biopsies are another important application of iMRI in those cases where the tumor is more readily seen in MR than in CT or ultrasound. [4,5,6]

Previously reported methods on slice to volume registration were mainly applied to the brain. [7,8,9] For the case of volume to volume registration, there are many reports of accurate voxel-based registration in the brain [10,11,12,13] and abdominal and pelvic organs.[1,14]

There are challenges to successful slice to volume registration for the prostate. They include:

1) A single slice, or a few slices, provides much less information than an entire volume for voxel based matching.

2) There is a low signal to noise ratio (SNR) in iMRI because of the emphasis on fast imaging typically with a low field scanner.

3) The pelvic region has irregular boundaries and can deform, unlike the brain to which registration has been most often applied. The prostate might move relative to the pelvic bones due to changes in rectal and bladder filling [15,16] or movement of the patient for treatment.

4) The normal prostate is a small organ that when healthy measures only about 3.8 cm in its widest dimension transversely across the base, [17] and the small prostate is located below a much larger bladder that can change shape and size.

5) The non-homogenous receive coil response can change from one acquisition to next.

We are investigating the use of voxel-based registration for this important application. We created a mutual information algorithm modified to include some features to improve robustness. We performed registration experiments under conditions found with low field open MR imaging.

2. REGISTRATION ALGORITHM

2.1. Similarity Measurement

Two similarity measurements, mutual information (MI) and correlation coefficient (CC), are used in our algorithm. The MI-based registration method is robust and suitable for multi-modality registration, is highly accurate for brain registration,[18] and is suitable for abdominal registration where there can be deformation.[1,14] However, the MI method has the problem of interpolation artifacts, which are especially serious in the case of down sampling in a multi-resolution approach.[19] Fortunately, CC produces fewer locally optimum values than does MI.[20] Our method combines both similarity measures to use the good attributes of each.

MI quantifies interdependency of two variables, such as image gray intensities of image A and B. When A and B are exactly aligned, MI is maximal.[18] We calculate MI using Equations 9 to 12 in the report by Maes et al.[18] CC is a measure of the relation between the statistical distributions of the two images. The absolute of CC has the range of 0 to 1. The higher the absolute value of CC, the more dependence the two images have.[21] We calculate CC using the equation 10 in the report by Rueckert et al.[21]

The algorithm shown in Figure 1 included special features to improve robustness for registration of MR prostate images. In the pseudo-code, the iMRI slice image is the *reference slice,* the slice image extracted from the high-resolution MRI volume is the *reformatted slice,* and the final reformatted slice is the *registered slice*. We used a multi-resolution approach and performed registration from low to high resolution. We used MI at the highest resolution because it gave a more robust solution, and we used CC at the lower resolutions because it gives few local optima and because it calculates faster than MI. We created a method to avoid local minima by restarting the registration with randomly perturbed parameters obtained from a uniform distribution about the very first initial guess. The algorithm restarts until the absolute CC between the reference and registered images is above a threshold or the maximum number of restarts is reached. Absolute CC is used for the restart test rather than MI because it has a well-defined range between 0 and 1 and because it provides an independent check of the MI result.

We used rigid body transformation (three translations and three rotations) and trilinear interpolation as described previously.[1] For optimization, we used the downhill simplex method of Nelder and Mead [22] and the Powell method,[23] but we prefer the former method as described later. Optimization of similarity ends either when the maximum number of calculations is reached (typically 500) or the fractional change in similarity function is smaller than a tolerance (typically 0.001). Our very first initial guess at the lowest resolution is all zeros for the 3 displacements and 3 angles. Based on our

Set an initial reformatted_slice in high-resolution MR volume and CC_thresholds

DO registration **FROM** lowest resolution **TO** highest resolution **BEGIN**

  Resample volume and slice to ¼, ½ or full number of voxels along linear dimension

  Initialize registration_results and number_restarts to zero for restarting registrations

  REPEAT

    Optimize similarity (CC^* or MI^{**}) between the reference slice and reformatted_slice

      1. **Transform** the initial reformatted_slice and **interpolate** to get a new reformatted_slice

      2. **Calculate** similarity between the reference slice and the new reformatted_slice

      3. **Repeat** 1 and 2 until meeting function tolerance or maximum iteration number

    Calculate CC between the reference slice and the optimal reformatted_slice

    Record CC, MI^{**} values and transformation parameters to registration_results

    Perturb the initial transformation parameters:

      initial_transformation_parameters = initial_transformation_parameters + random • factor

    Trace the number of restarts: number_restarts = number_restarts + 1

  UNTIL (CC > CC_threshold) **OR** (number_restarts > maximum_restarts)

  Select the final transformation_parameters based on CC^* or MI^{**} among registration_results

  Scale the parameters and **assign** to initial_transformation_parameters of next higher resolution

END

Figure 1. Registration algorithm. Capital bold words are computer language.   The outer loop from DO to END gives the multi-resolution approach. The inter loop from REPEAT to UNTIL is for restarting registration. Registration_results and number_restarts are used to store temporary values in the program. See text for details.
[*] CC is used at lower resolutions, ¼ or ½ number of voxels.
[**] MI is used only at high resolution, full number of voxels.

experience, we set the CC thresholds at 0.60, 0.65 and 0.70, and the maximum numbers of restarts at 25, 15, and 5, from low to high resolution, respectively.

In Figure 1, there are several differences between low and high resolutions. At lower resolutions, we resample the volume and slice to 1/4 or 1/2 size along the linear dimension. We optimize the CC between reference and reformatted slices to obtain optimal transformation parameters. We record important results such as all CC optimized values, the number of restarts, and the transformation parameters following an optimization. At the end of either of these resolutions, we select the transformation parameters that have the maximum CC value. We then scale the parameters and assign them to be initial values at the next higher resolution. At the highest resolution, MI instead of CC is chosen to be the similarity measurement method, and we select the final transformation parameters with maximum MI instead of CC.

There are several preprocessing details. The input MRI volumes are 256 x 256 x 128 voxels that have an almost isotropic size over a field of view covering the whole pelvis. Isotropic voxels are created using 3D linear interpolation or higher order interpolation methods.[1]

3.   EXPERIMENTAL METHODS

3.1.   Data Acquisition

All MRI volumes were acquired using a 1.5 T Siemens MRI system (Magnetom Symphony, Siemens Medical Systems in Erlangen, Germany). An 8-element phased array body coil was used to ensure coverage of the prostate with a uniform sensitivity. Typically two anterior and two posterior elements were enabled for signal acquisition. We used a 3D PSIF sequence with 9.4/5.0/60 (TR/TE/flip) yields 160 x 256 x 128 voxels over a 219 x 350 x 192-mm rectangular FOV and 1.37 x 1.37 x 1.5-mm voxels oriented to give the highest resolution for transverse slices. There is over-sampling at 31% in

the slice direction to reduce aliasing artifacts. This sequence gave excellent image contrast for the prostate and its surroundings.

3.2.   Creation of Images for Testing

To test the ability of the slice-to-volume (SV) registration, we obtained high-resolution MRI volumes and simulated iMRI images by adding noise and receive coil inhomogeneity. We compared SV registration to volume-to-volume (VV) registration results.

We simulated iMRI slice images. We averaged 3 slices together to simulate an iMRI 4-mm thick slice. We used a homogenous phantom to measure the SNR of iMRI images on our 0.2 T open magnet system (Magnetom Open, Siemens Medical Systems in Erlangen, Germany). We used simulated iMRI images to test the dependence of registration on noise levels.   Figure 2 shows the simulated iMRI slice images.

3.3.   Registration Experiments

We acquired high-resolution MR volumes from three volunteers. Each has two pairs of volumes for registration. We extracted three slices from one volume and used these slices to simulate an iMRI image. We tested multiple ways to acquire slices for SV registration. First, we used transverse, sagittal and coronal slices for registration, respectively. The objective was to optimize the slice orientation for image guidance. Second, we extracted slices from different positions such as centered at the prostate, and above and below the prostate by 35 mm. This experiment was performed to investigate the range for reliable slice registration. Third, we tested the dependence of the registration on noise levels.
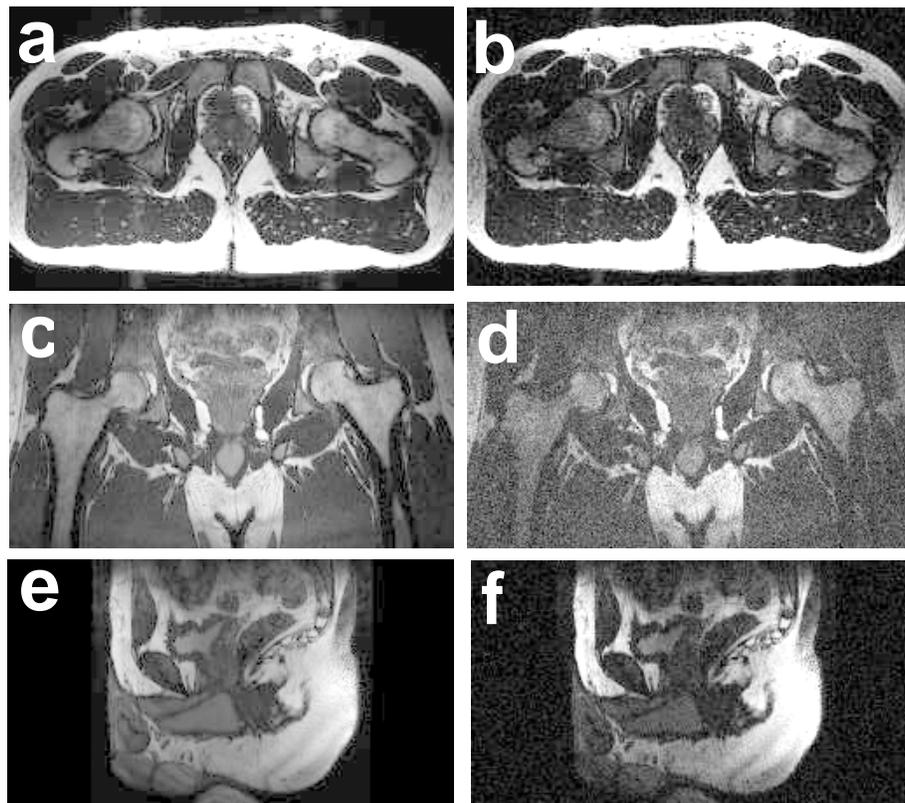
Figure 2. Simulated iMRI images. Images on the left, (a), (c) and (e), are the high-resolution MR images in transverse, coronal and sagittal planes, respectively. Images on the right are corresponding simulated iMRI images with SNR = 8. The images are of volunteer V2.
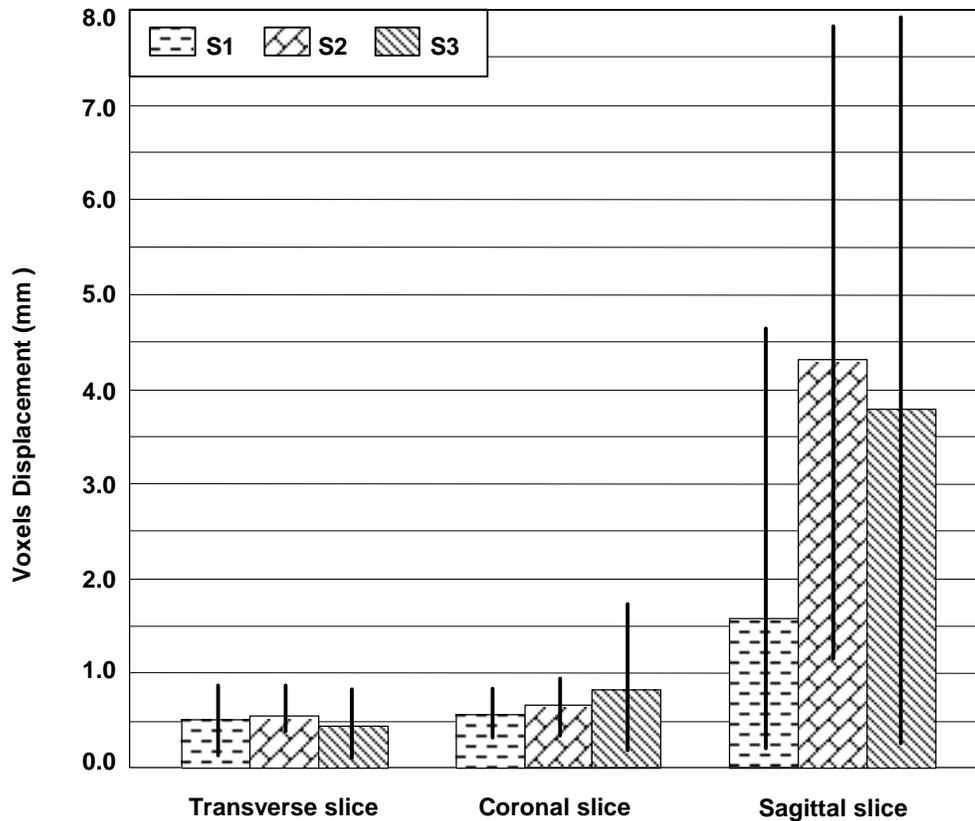
Figure 3. SV registration using slices at different orientations. The error metric is voxel displacement between the SV and VV results. Plotted are mean errors as well as maximums and minimums that show the spread of the data. S1, S2, and S3 refer to volunteers. Each volunteer has two volume pairs. For each pair, five transverse slices centered at the prostate were extracted from one volume and registered to the other. The same procedures were applied to coronal and sagittal slices.

3.4.   Evaluation Methods

To test the program, we transformed a reference volume using known parameters to obtain a *digital phantom*. We extracted slices from the digital phantom and registered them to the reference volume. Because the transformation was known, we could validate the performance of the software.

Our standard evaluation method was to compare SV and VV registration. The VV registration accuracy was previously evaluated to be on the order of one voxel (1.37 mm) [14]. We defined a volume of interest (VOI) just covering the prostate and applied the transformations obtained by VV and SV registrations to voxels within the VOI.   We calculated the 3D displacement on a voxel-by-voxel basis over the two transformed VOIs. The mean voxel displacement was used as our metric of SV registration error.

4.   RESULTS AND DISCUSSIONS

More than 300 SV registration experiments were performed under a variety of conditions expected for applications in iMRI-guided treatment of the prostate. First, we report the effect of slice orientation and position on registration. Second, we describe the results associated with image noise. At the end, we describe some details on the algorithm implementation.
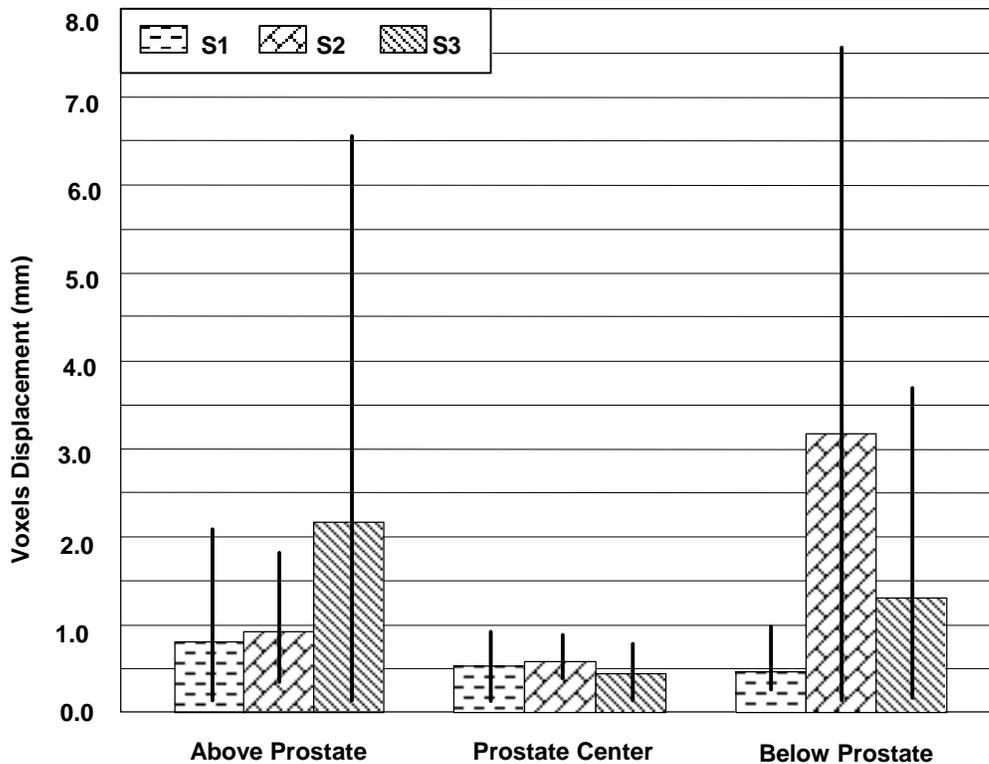
Figure 4. SV registration using transverse slices at different positions. Relative to the prostate, five iMRI slices each were extracted near its center, ≈ 35 mm above its center, and ≈ 35 mm below its center. Other details are given in Figure 3. Slices at the prostate center work best.

4.1. Slice Orientation and Position

Figure 3 shows registration results for single slices oriented in different directions. All slices intersect the prostate. Transverse slices give the lowest average error across the three volunteers, 0.39 ± 0.19 mm. The reason for this result is that a transverse slice contains more anatomical structures than do slices in other orientations. A transverse slice also excludes the bladder and portions of the rectum that can deform and create inconsistent matches for registration. The following analyses are all based on transverse slices.

Figure 4 shows registration results for transverse slices at different heights relative to the prostate. Slices centered on the prostate produced the best results with the displacement error always being less than 1.0 mm. On the one hand, slices centered at the prostate are good because they include an abundance of bony structures that provide adequate information for registration. Slices above the prostate include the bladder, which can deform and stress the registration algorithm. Slices below the prostate mainly contain fatty regions from the hips that can also deform and have less information for registration.

4.2. Noise Level and Robustness

We performed preliminary experiments using different noise levels in the simulated iMRI images. When SNR values were 30, 15 and 5, registration errors were always less than 0.9 mm for three volunteers in all conditions. For more than 200 registration experiments, the algorithm was very robust and never failed even with these large noise values. We believe the algorithm to be insensitive to noise.

4.3. Program Implementation

We implemented the registration program using IDL (Interactive Data Language, Research System Inc., Boulder, CO.). The time for an SV registration, typically 40 to 90 sec on a Pentium III, 800 MHz CPU, with 512 Mbytes of memory, could

be improved using optimized C code rather than IDL. The simplex optimization method worked faster than the Powell method in our implementation. This result is contrary to our previous experience.[1] We think that this phenomenon occurred because the Powell method depends on the order that parameters are optimized. Because we do not require preprocessing to determine initial values, there are no clear choices for which parameters to optimize first. Each call to the Simplex optimization for restarts or optimization at a finer resolution resulted in 50 to 105 similarity evaluations before the tolerance value (0.001) was reached.

The restarting and multi-resolution features are important. Using normal clinical transverse images covering the prostate, the algorithm always gave very nearly the same transformation parameters (less than 0.01 voxels and 0.01 degrees) using a wide variety of initial guesses. The multi-resolution approach enabled the program to get close to the final value quickly because of the reduced number of calculations. Although serious motion artifacts may stress the registration, our experience is that these can be controlled with appropriate subject compliance and with the proper acquisition technique. Organ motion and deformation from one acquisition to the next are other factors that can affect the performance of the algorithm, especially when subject is in a different position or there is rectal and bladder filling. [14] Again, our experience is that these errors can be controlled. [14]

5. CONCLUSION

The automatic slice-to-volume mutual information registration algorithm was quite robust for transverse slice images covering the prostate. There were no registration failures in over 200 experiments on MRI images without obvious artifacts. The registration error of < 1.0 mm should be sufficiently accurate to aid in the application of iMRI-guided minimal invasive thermal ablation of prostate cancer. We are beginning to explore these applications in clinical procedures and animal experiments.

ACKNOWLEDGEMENTS

REFERENCES

1. A. Carrillo, J. L. Duerk, J. S. Lewin, and D. L. Wilson, "Semiautomatic 3-D image registration as applied to interventional MRI liver cancer treatment," *IEEE Trans. Med. Imag.,* vol. 19, no. 3, pp. 175-185, Mar. 2000
2. J. S. Lewin, C. F. Connell, J. L. Duerk, Y. C. Chung, M. E. Clampitt, J. Spisak, G. S. Gazelle, and J. R. Haaga, "Interactive MRI-guided radiofrequency interstitial thermal ablation of abdominal tumors: clinical trial for evaluation of safety and feasibility," *JMRI*, vol. 8, no.1, pp. 40-47, Jan. 1998.
3. E. M. Merkle, J. R. Shonk, J. L. Duerk, G. H. Jacobs, and J. S. Lewin, "MR-guided RF thermal ablation of the kidney in a porcine model," *Am. J. Roentgenol.*, vol.173, no. 3, pp. 645-651, Sep, 1999.
4. K. Kagawa, W.R. Lee, T. E. Schultheiss, M. A. Hunt, A. H. Shaer, G. E. Hanks, "Initial clinical assessment of CT-MRI image fusion software in localization of the prostate for 3D conformal radiation therapy," *Int. J. Radiation Oncology Biol. Phys.,* vol. 38, no. 2, pp. 319-325, 1997.
5. M. Milosevic, A. Voruganti, R. Blend, H. Alasti, P. Warde, M. McLean, P. Catton, C. Catton, M. Gospodarowicz, "Magnetic resonance imaging (MRI) for localization of the prostatic apex: comparison to computed tomography (CT) and urethrography," *Radiotherapy and Oncology,* vol. 47, no.3, pp. 277-284, Jun. 1998.
6. R.A.H. Boni, J.A. Boner, J.F. Debatin, F. Trinkler, H. Knonagel, A. Vonhochstetter, U. Helfenstein, G.P. Krestin, **"**Optimization of prostate carcinoma staging - comparison of imaging and clinical methods," *Clinical Radiology*, vol. 50, no. 9, pp. 593-600, Sep. 1995
7. B. Kim, J.L. Boes, P.H. Bland, T.L. Chenevert, C.R. Meyer, "Motion correction in fMRI via registration of individual slices into an anatomical volume," *Magnetic Resonance in Medicine*, vol. 41, pp. 964-972, 1999.

8. T.S. Kim, M. Singh, W. Sungkarat, C. Zarow, H. Chui, "Automatic registration of postmortem brain slices to MRI reference volume," *IEEE Trans. Nuclear Science*, vol. 47, no. 4, Aug. 2000.

9. J. Zhengping, P.H. Mowforth, "Mapping between MR brain images and a voxel model," *Medical Informatics*, vol. 16, no. 2, pp. 183-193, Apr-Jun., 1991

10. D.L.G. Hill, L.A. Langsaeter, P.N. Poynter-Smith, C.L. Emery, P.E. Summers, S.F. Keevil, J.P.M. Pracy, R. Walsh, D.J. Hawkers, M.J. Gleeson, "Feasibility study of magnetic resonance image-guided intranasal flexible miroendoscopy," *Computer Aided Surgery*, vol. 2, pp. 264-275, 1997.

11. P. A. Freeborough, R. P. Woods, and N. C. Fox, "Accurate registration for 3D MR brain images and its application to visualizing change in neurodegenerative disorders," *J CAT,* vol. 20, no. 6, pp. 1012-1022, 1996.

12. M. Holden, D. L. G. Hill, E. R. E. Denton, J. M. Jarosz, T. C. S. Cox, T. Rohlfing, J. Goodey, D. J. Hawkes, "Voxel similarity measures for 3-D serial MR brain image registration," *IEEE Trans. Med. Imag.,* vol. 19, no. 2, pp. 94 – 102, Feb. 2000

13. R.W. Cox, A. Jesmanowicz, "Real-time 3D image registration for functional MRI," *Magnetic Resonance in Medicine*, vol. 42, pp. 1014-1018, 1999.

14. B.W. Fei, A. Wheaton, Z. Lee, J.L. Duerk, and D.L. Wilson, "Registration of MR images of the prostate," Submitted to *IEEE Trans. Med. Imag.,* Jan. 2001.

15. M.V. Herk, A. Bruce, A.P.G. Kroes, T. Shouman, A. Touw, J.V. Lebesque, "Quantification of organ motion during conformal radiotherapy of the prostate by three dimensional image registration," *Int. J. Radiation Oncology Biol. Phys.,* vol. 33, no. 5, pp. 1311-1320, 1995.

16. R.K. Ten Haken, J.D. Forman, D.K. Heimburger, A. Gerhardsson, D.L. McShan, C. Perez Tamayo, S.L. Schoeppel, A.S. Litchter, "Treatment planning issues related to prostate movement in response to differential filling of the rectum and bladder," *Int. J. Radiation Oncology Biol. Phys.,* vol. 20, no. 6, pp. 1317-1324, Jun. 1991.

17. H. Gray, T. Pickering Pick, R. Howden, "Gray Anatomy: The classic collector's edition," New York: Gramercy Books, 1977, p. 1010.

18. F. Maes, A. Collignon, D. Vandermeulen, G. Marchal, P. Suetens, "Multimodality image registration by maximization of mutual information," *IEEE Trans. Med. Imag.,* vol. 16, no.2, pp. 187 –198, April 1997

19. J.P.W. Pluim, J.B.A. Maintz, M.A. Viergever, "Interpolation artifacts in mutual information-based image registration," *Computer vision and image understanding*, vol. 77, no.2, pp. 211-232, Feb. 2000

20. B.W. Fei, Z. Lee, J.L. Duerk, and D.L. Wilson, "Slice to volume registration as applied to interventional MRI-guided treatment of prostate cancer," In preparation.

21. D. Rueckert, L. I. Sonoda, C. Hayes, D. L. G. Hill, M.O. Leach, D. J. Hawkes, "Nonrigid registration using free-form deformations: application to breast MR images," *IEEE Trans. Med. Imag.,* vol. 18, no. 8, pp. 712 –721, 1999

22. J. Nelder and R.A. Mead, "A simplex method for function minimization," *Comp. J.*, vol. 7, pp. 308-313, 1965

23. M. J. D. Powell, "An iterative method for finding stationary values of a function of several variables," *Comp. J.*, vol. 5, pp. 147-151, 1962

Baowei Fei, Andrew Wheaton, Zhenghong Lee, Kenichi Nagano, Jeffrey L. Duerk, and David L. Wilson, "Robust registration method for interventional MRI-guided thermal ablation of prostate cancer", Seong Kim Mum, Editor, Proc. SPIE 4319, 53 (2001)